

86835  
p. 10

NASA Technical Memorandum 105329  
ICOMP-91-22

# A Two-Dimensional Euler Solution for an Unbladed Jet Engine Configuration

Mark E.M. Stewart  
*Institute for Computational Mechanics in Propulsion*  
*Lewis Research Center*  
*Cleveland, Ohio*

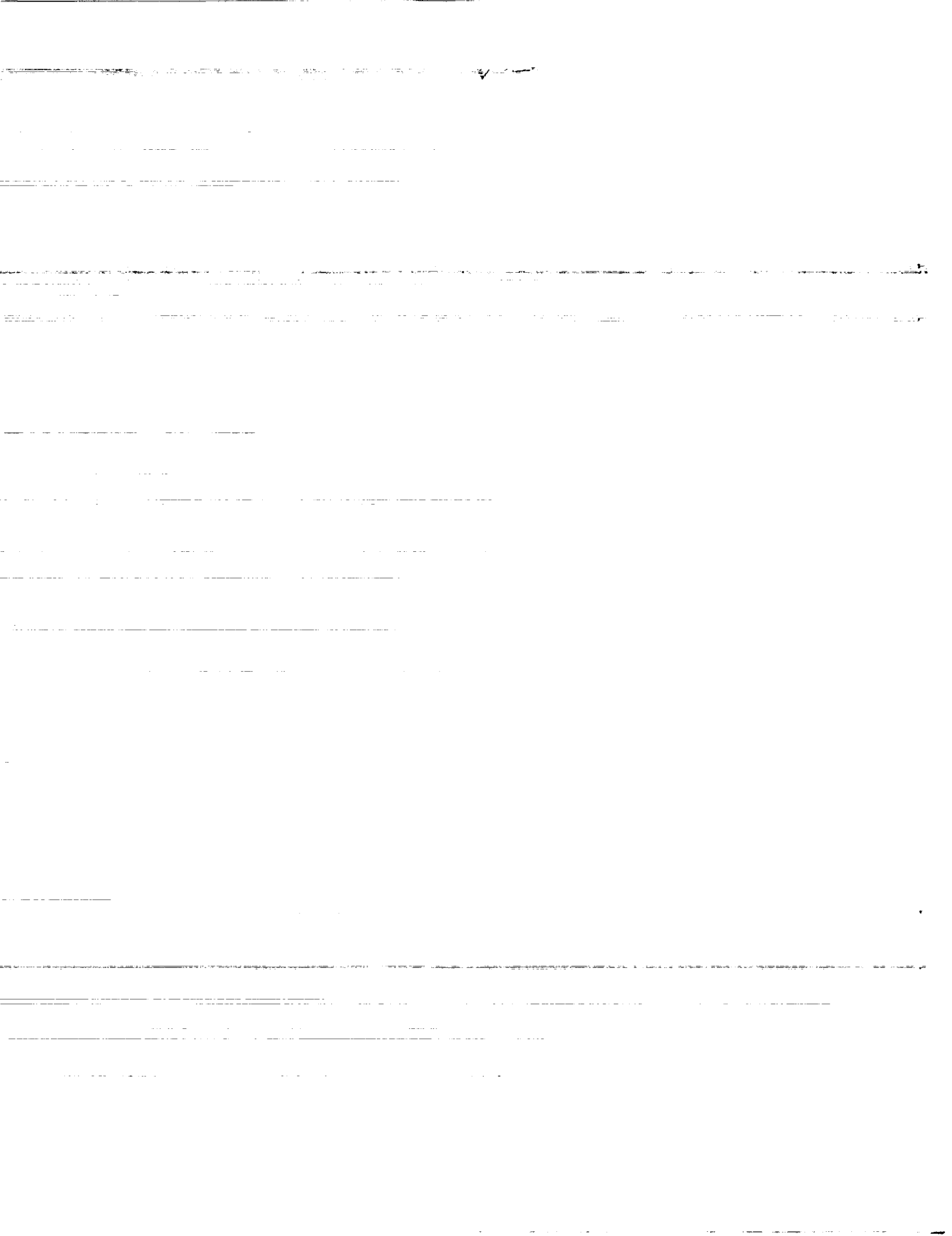
Prepared for the  
Third Canadian Symposium on Aerodynamics  
sponsored by the Canadian Aeronautics and Space Institute  
Toronto, Canada, November 20-21, 1991



(NASA-TM-105329) A TWO-DIMENSIONAL EULER  
SOLUTION FOR AN UNBLADED JET ENGINE  
CONFIGURATION (NASA) 10 p CSCL 200

N92-23560

Unclas  
G3/34 0086835



# A TWO-DIMENSIONAL EULER SOLUTION FOR AN UNBLADED JET ENGINE CONFIGURATION

Mark E. M. Stewart  
Institute for Computational Mechanics in Propulsion  
NASA Lewis Research Center

## SUMMARY

A two-dimensional, nonaxisymmetric Euler solution in a geometry representative of a jet engine configuration without blades is presented. The domain, including internal and external flow, is covered with a multiblock grid. In order to construct this grid, a domain decomposition technique is used to subdivide the domain, and smooth grids are dimensioned and placed in each block. The Euler solution is verified by examining five theoretical properties. The result demonstrates techniques for performing numerical solutions in complex geometries and provides a foundation for complete engine throughflow calculations.

## NOMENCLATURE

$C_D$	drag coefficient	$t$	time
$C_L$	lift coefficient	$u, v$	velocity components
$D( )$	artificial dissipation	$vol$	volume
$E$	total energy	$w$	vector of dependent variables
$n$	surface normal	$\alpha$	angle of attack
$H$	total enthalpy	$\gamma$	ratio of specific heats
$P$	pressure	$\rho$	density
$Q( )$	flux integral approximation	$\sigma_i$	stage coefficients
$s$	surface area	$\Omega$	arbitrary region

## INTRODUCTION

Numerical simulations have provided valuable insights into a wide range of important problems in science and engineering. In aeronautical engineering these applications range from fundamental problems in fluid mechanics to practical problems in design. Simulations have helped reduce design time while improving designs, and they are now an integral part of the design process.

Traditionally, jet engine research and development has involved a substantial experimental component. Engineering practice for engine development in the 1980's involved preliminary analysis and computer modeling of the first-order physical effects followed by extensive experimental testing of engine components in isolation. This effort was followed by engine integration based on component performance and culminated in ground testing of the integrated engine. The process is expedited by experience and extensive databases of test data, which allow estimates of physical effects including endwall boundary layer losses and shock losses. However, this development and integration can cost hundreds of millions of dollars, and it can be years before the viability of a design is firmly established. In order to reduce the risks of this process, design changes are often incremental and build on experience, and because of these risks, radical designs are difficult to fully test.

Computational methods are available that complement experimental techniques in the analysis of engine flow phenomena. For isolated blade rows inviscid and viscous codes have been developed. Dawes<sup>1</sup> as well as Chima and Yokota<sup>2</sup> have reported codes for three-dimensional viscous flow in a blade row. Whitfield et al.<sup>3</sup> have demonstrated techniques for time-accurate simulations of counterrotating propfans.

In multistage compressors and turbines today's algorithms and computers dictate the use of physical modeling because of the geometrical complexities of relatively moving blade rows and the physical effects of their interactions. A foundation of compressor throughflow calculations is the work of Wu<sup>4</sup> who has presented an approach to solving quasi-three-dimensional flow by using a meridional surface coupled with a blade-to-blade surface. Jennions and Stowe<sup>5,6</sup> have demonstrated a throughflow calculation for a turbine blade. Wisler et al.<sup>7</sup> have mentioned the use of circumferentially averaged throughflow calculations for evaluating compressor designs. Recently, a number of techniques have been introduced for three-dimensional multistage calculations. Denton<sup>8</sup> has presented an Euler calculation for multistage turbomachines, and Dawes<sup>9</sup> has reported a three-dimensional viscous technique. To model flow in a multistage machine, Adamczyk et al.<sup>10</sup> have developed a combination of space- and time-averaging operators in the spirit of Reynolds averaging.

Despite the complexities of simulating components, they do not operate in isolation and their interactions are important. Yet, in engine development, components are integrated on the basis of their performance in isolation. With predictive tools largely limited to one-dimensional analysis of complete engines, designs must be conservative even when there is a need for less conservative designs that require consideration of these interaction effects.

The goal of the current work is to lay a foundation for complete engine throughflow calculations. As a step in this task the current calculation deals with the geometrical and numerical problem of solving for the external and internal flow in the inlet, bypass duct, core duct, and nozzle of the engine configuration. The geometry is not axisymmetric in that there is a uniform depth over the computational domain instead of radial variation. Given this foundation, determination of the axisymmetric unbladed solution will follow.<sup>11</sup> A further step is modeling blade effects in the solution.

First, the task of determining the contours for this geometrical configuration is detailed. Then the techniques for finding a multiblock grid within the domain are presented. Finally, the numerical methods are explained and solution results and their verification are presented.

## GEOMETRY MODELING

The geometry for this problem is based on the Energy Efficient Engine ( $E^3$ ), which was designed and tested by General Electric for NASA in the early 1980's. In particular, the geometry is based on the ground test of the integrated engine. The engine was designed for use in commercial jets in the 1990's.

Several modifications were made to the geometry; the most important was neglecting blade effects in the compressor and turbine sections. The compressor does work and compresses the air passing through the engine core, and for the actual engine the pressure ratio is 23:1. After passing through the combustor, where there is an enthalpy increase, the flow expands through turbine blades, which remove energy from the flow to drive the compressor and the fan. In this

solution these effects were neglected, and the compressor, combustor, and turbine sections were replaced with a duct. However, a duct with a comparable area ratio through these sections will produce sonic flow at the throat even at relatively low Mach numbers. A shock at the throat limits mass flow through the engine core, and changes the streamlines throughout the engine. In order to reduce this problem the core area ratio was changed to 2:1 by raising the splitter plate.

Several other modifications were made to the geometry contours. Since the geometry was for a ground test, an external nacelle was designed by using standard design practices. Furthermore, a small splitter island near the core bypass was excluded. Since surface pressure is very sensitive to the smoothness of the surface contours, every effort was made to ensure continuity of the surfaces and their derivatives. In particular, least-squares curve fitting to a set of sine and cosine basis functions has been used to remove high-frequency errors in the coordinate data.

## GRID GENERATION

The grid on which the calculation is done is a multiblock grid that consists of block-structured grids which cover the domain without overlapping. The interfaces between blocks are matched so that coordinate lines pass from one block to another continuously without a slope discontinuity. These grids are generated by using the TOPOS program<sup>12</sup>, which finds a domain decomposition, dimensions the grids within the blocks, and places smooth grids within each block.

The domain decomposition is determined with an algorithm that finds boundary-conforming regions within a domain. In a way analogous to how the skin of a balloon conforms to neighboring walls when blown up in a confined space, this algorithm finds topologically rectangular regions within the domain. If this region is removed from the domain to produce a truncated domain, the algorithm may be applied again to find a further block. By repeated application of the algorithm, the domain is reduced until it is covered.

Once a domain decomposition has been found, transformations may be applied to cut and split the decomposition and change its topology. The transformations are isomorphic with respect to the data structures used to represent the domain decomposition. These transformations, with their isomorphic properties, provide a valuable tool for manipulating domain decompositions.

The dimensions of each grid block are found so that coordinate lines continue through each block interface. Since the block topology is globally unstructured, this interface property places a nontrivial constraint on the grid dimensions. However, these properties may be formulated as a system of underconstrained linear equations with constant, integer coefficients that require positive integer solutions. If the system of equations admits a solution, this solution can be found with the simplex linear programming algorithm.<sup>13</sup> Furthermore, the simplex method specifies some of the parameters in this system of equations that may be varied to adapt the grid. Smooth grids are then placed in these dimensioned blocks by using a Coons patch followed by smoothing with an elliptic grid generator.

## NUMERICAL METHODS

The two-dimensional Euler equations model inviscid, compressible flow and are given by

$$\frac{d}{dt} \int_{\Omega} w \, dVol = - \oint_{\partial\Omega} F \cdot n \, ds \quad (1)$$

where  $F = (f, g)$  and

$$w = \begin{pmatrix} \rho \\ \rho u \\ \rho v \\ \rho E \end{pmatrix} \quad f(w) = \begin{pmatrix} \rho u \\ \rho u^2 + P \\ \rho uv \\ \rho uH \end{pmatrix} \quad g(w) = \begin{pmatrix} \rho v \\ \rho uv \\ \rho v^2 + P \\ \rho vH \end{pmatrix}$$

$$P = (\gamma - 1) \left( \rho E - \frac{\rho(u^2 + v^2)}{2} \right) \quad H = \frac{\gamma}{(\gamma - 1)} \frac{P}{\rho}$$

Here  $\gamma = 1.4$ . The numerical approximation and solution techniques are based on the FLO52 program of Jameson et al.<sup>14</sup> The discretization of these equations on the grid takes  $\Omega$  to be a cell, and the flux through each face is approximated from the centroid-based dependent variables as

$$\int_{face} f \, dy - g \, dx \cong \frac{1}{2} (f_M + f_N, g_M + g_N) \cdot (\Delta y_{face}, -\Delta x_{face}) \quad (2)$$

where  $M$  and  $N$  are cells adjacent to the face. The discretized equations for each cell are advanced to a steady state by a multi-stage scheme,

$$\begin{aligned} w^{(1)} &= w_i + \sigma_1 \Delta t [Q(w_i) + D(w_i)] \\ w^{(2)} &= w_i + \sigma_2 \Delta t [Q(w^{(1)}) + D(w^{(1)})] \\ w^{(3)} &= w_i + \sigma_3 \Delta t [Q(w^{(2)}) + D(w^{(1)})] \\ w^{(4)} &= w_i + \sigma_4 \Delta t [Q(w^{(3)}) + D(w^{(1)})] \\ w_{i+1} &= w_i + \sigma_5 \Delta t [Q(w^{(4)}) + D(w^{(1)})] \end{aligned} \quad (3)$$

where  $\sigma_i$  are stage coefficients,  $Q(w)$  is the convective flux approximation for the cell given in equation (2), and  $D(w)$  is an artificial dissipation. The artificial dissipation consists of third-order dissipation, which stabilizes the time-stepping scheme, and first-order dissipation, which is switched on near shocks to capture them.

Three types of boundaries can occur in a grid. First, at solid surfaces a free-slip, tangential flow condition is applied. Second, at the truncation boundary in the far field the free-stream conditions are matched to internal conditions by matching incoming and outgoing Riemann invariants. Third, at the interface boundary between blocks information must be exchanged. Since coordinate lines pass through these boundaries continuously, the continuation of one grid into its neighbor is trivial. Each grid in computational space has a layer of cells surrounding it, where dependent variable values from the continuation onto the neighboring grid may be placed. Then the convective flux  $Q(w)$  and the artificial dissipation  $D(w)$  are calculated, as usual, in each cell within the grid. By using this scheme and passing dependent variables across block interfaces at each stage of equation (3), the solution is not influenced by these block interfaces regardless of how the domain is decomposed.

Several techniques are used to enhance the convergence of equation (3). Since there are no blades that do work on the flow, the solution is isenthalpic and enthalpy damping<sup>15</sup> may be used to enhance convergence. Since a steady-state solution to equation (1) is sought, the maximum local time step permitted by the CFL condition is used. Consequently, the simulation is not limited by a small time step determined by the smallest cell in the grid.

A multigrid algorithm<sup>16</sup> is used to accelerate convergence further. The multigrid levels are constructed by finding the coarsest grid that does not have excessive stretching or high aspect ratios due to the nonuniformity of the decomposition topology. Each dimension of this coarse grid is multiplied by a power of 2 to construct finer grid levels. In the current calculation the grid topology and coarsest grid allow three grid levels to be used and this improves convergence considerably. For each grid level added, the convergence rate, measured by the average density residual, increases by about a factor of 2.

## RESULTS

The grid on which the calculation has been done is shown in figure 1, where the bold lines indicate the interfaces between blocks. The grid contains 16800 cells in 10 blocks that cover the external field, inlet, bypass duct, core duct, and nozzle of the nonaxisymmetric engine configuration.

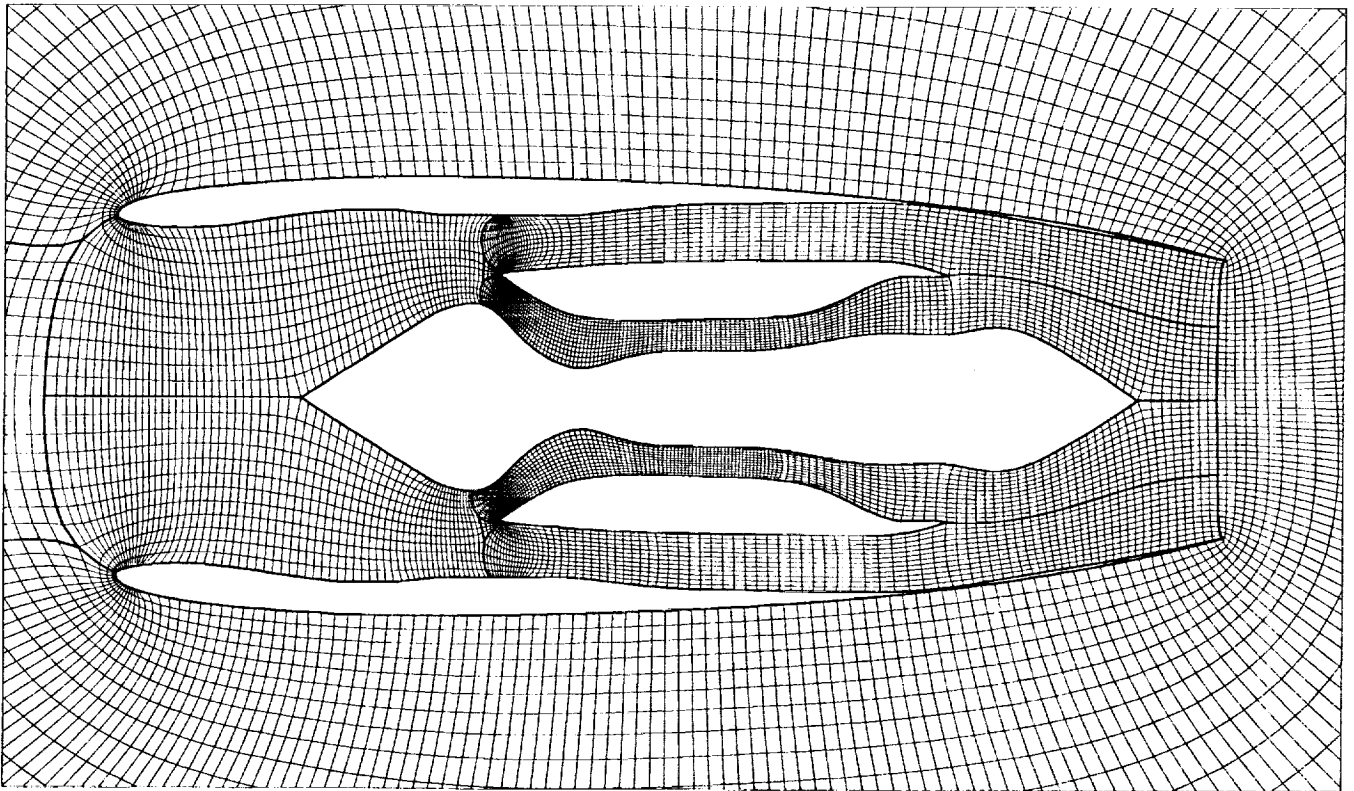


Figure 1: Inner grid for jet engine configuration.

The geometry is symmetric about the meanline of the hub, but the grid is not since there is no symmetry condition applied to the grid between the two halves. With a symmetric grid at zero angle of attack the solution would be exactly symmetric and measures of the solution, such as the lift coefficient would exactly cancel. However, with an asymmetric grid the solution will not necessarily be symmetric, and the lift coefficient will not necessarily be zero. Consequently, this grid asymmetry can be exploited to verify the resolution of the solution.

The simulation was run 2500 iterations at Mach 0.3 and  $0^\circ$  angle of attack. The convergence history is shown in figure 2. The single-grid convergence history is also shown to demonstrate the speedup due to multigrid.

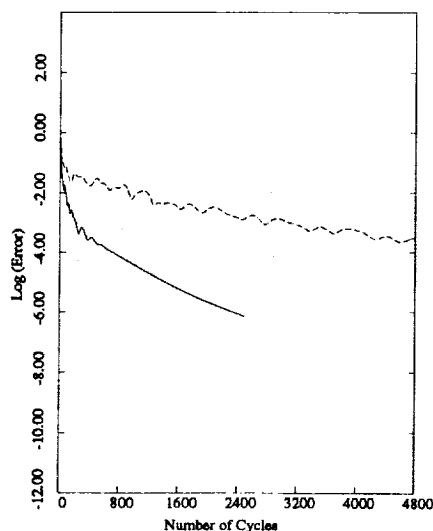


Figure 2: Convergence histories of average density residual with two multigrid levels (solid line) and without multigrid (dashed line).

There are no known experimental results for comparison, but the simulation may be verified on the basis of five theoretical quantities. First, the solution conserves mass and energy. Conservation of mass is directly demonstrated in figure 2 by the convergence of the average density residual  $|\frac{d\rho}{dt}|$  over the domain. Conservation of energy follows from convergence of the average total energy residual  $|\frac{d\rho E}{dt}|$  over the domain. Second, since the angle of attack,  $\alpha$ , is zero and the geometry is symmetric, the lift coefficient,  $C_L$ , should be zero. It is calculated to be  $C_L = -0.0031$ . The deviation from zero is due to the asymmetry of the grid, the truncation error in the convective flux approximation  $Q(w)$ , and the artificial dissipation  $D(w)$ . Third, since the solution is subcritical, the drag coefficient  $C_D$  should be zero. It is calculated to be  $C_D = 0.0045$ . Again, the deviation from zero is due to the asymmetry of the grid, error in the approximation of  $Q(w)$ , and the artificial dissipation  $D(w)$ . Fourth, since inviscid, adiabatic flow is isentropic, deviations from constant entropy are a further test. Over the surfaces of the body the entropy deviations are less than 0.5 percent. The large deviations are at the leading edge of the splitter plate with its small leading-edge radius, at the curved inlet to the core passage, and at the leading edge of the nacelles.



Fifth, the asymmetry of the grid does not guarantee a symmetric solution. Figure 3 shows the pressure distributions over the symmetric surfaces of the components. Surface pressure is sensitive to errors, and the result shows symmetry since surface pressure overplots on the symmetric surfaces. The largest deviation is in the core passage and is attributed to an accumulation of error as the flow passes through the core duct.

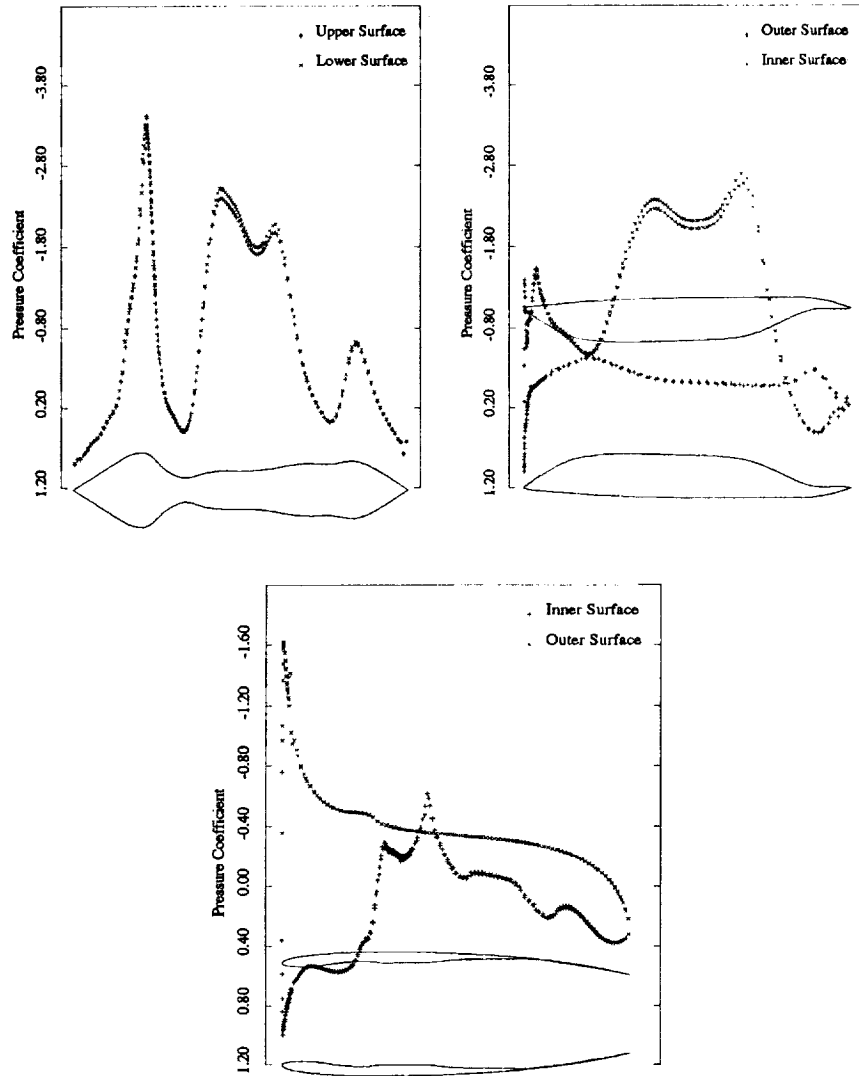


Figure 3: Normalized pressure distributions over the symmetric surfaces. Clockwise from top left, the components are the hub, the splitter plate, and the nacelle.

### CONCLUSIONS

A two-dimensional, nonaxisymmetric Euler solution for a jet engine geometry has been presented. The multiblock grid is generated by using techniques that find a domain decomposition and a grid within the domain. The solution has been verified on the basis of five theoretical quantities. These results demonstrate a foundation on which further simulations can be built, including solutions for axisymmetric configurations and solutions with blade effects included.

## ACKNOWLEDGEMENTS

The author would like to thank Andy Kuchar of General Electric Aircraft Engines for providing the hot flowpath coordinates for the ICLS ground test. John Abbott and Chuck Putt have provided considerable assistance with the geometry specification. Gregory Swartwout has cheerfully kept the computers running. The flow code is based on the FLO52 code of Antony Jameson. Joseph Mathew, Jeffrey Yokota, and John Adamczyk have provided valuable advice and insights.

## REFERENCES

- <sup>1</sup> Dawes, W. N., "A Numerical Analysis of the Three-Dimensional Viscous Flow in a Transonic Compressor Rotor and Comparison With Experiment," Journal of Turbomachinery, vol. 109, no. 1, Jan. 1987, pp. 83-90.
- <sup>2</sup> Chima, R. V. and Yokota, J. W., "Numerical Analysis of Three-Dimensional Viscous Internal Flows", AIAA Journal, vol. 28, no. 5, May 1990, pp. 789-806.
- <sup>3</sup> Whitfield, D., Swafford, T., Mulac, R., Belk, D. and Janus, J., "Three-Dimensional Unsteady Euler Solutions for Propfans and Counter-Rotating Propfans in Transonic Flow," AIAA Paper 87-1197, June 1987.
- <sup>4</sup> Wu, C. H., "A General Theory of Three-Dimensional Flow in Subsonic and Supersonic Turbomachines of Axial-, Radial-, and Mixed-Flow Types," NACA-TN 2604, 1952.
- <sup>5</sup> Jennions, I. and Stowe, P., "A Quasi-Three-Dimensional Turbomachinery Blade Design System: Part I—Throughflow Analysis," ASME Journal of Engineering for Gas Turbines and Power, vol. 107, no. 2, April 1985, pp. 301-307.
- <sup>6</sup> Jennions, I. and Stowe, P., "A Quasi-Three-Dimensional Turbomachinery Blade Design System: Part II—Computerized System," ASME Journal of Engineering for Gas Turbines and Power, vol. 107, no. 2, April 1985, pp. 308-316.
- <sup>7</sup> Wisler, D. C., Koch, C. C. and Smith, L. H., "Preliminary Design Study of Advanced Multistage Axial Flow Core Compressors," NASA CR-135133, 1977.
- <sup>8</sup> Denton, J. D., "The Calculation of Three Dimensional Viscous Flow Through Multistage Turbomachines," ASME Paper 90-GT-19, June 1990.
- <sup>9</sup> Dawes, W. N., "Towards Improved Throughflow Capability—The Use of 3D Viscous Flow Solvers in a Multistage Environment," ASME Paper 90-GT-18, June 1990.
- <sup>10</sup> Adamczyk, J. J., Mulac, R. A. and Celestina, M. L., "A Model for Closing the Inviscid Form of the Average-Passage Equation System," ASME Paper 86-GT-227, June 1986 (Also, NASA TM-87199.)
- <sup>11</sup> Stewart, M. E. M., "Euler Solutions for Unbladed Jet Engine Configurations," AIAA Paper 92-0544, Jan. 1992 (Also, NASA TM-105332.)
- <sup>12</sup> Stewart, M. E. M., "Non-Overlapping Composite Meshes for Multi-Element Airfoils," Ph. D. Thesis, Princeton University, 1990.
- <sup>13</sup> Press, W. H., Flannery, B. P., Teukolsky, S. A. and Vetterling, W. T., "Linear Programming and the Simplex Method," Numerical Recipes in C: The Art of Scientific Computing, 1st ed., Cambridge University Press, Cambridge, 1988, pp. 329-343.
- <sup>14</sup> Jameson, A., Schmidt, W. and Turkel, E., "Numerical Solution of the Euler Equations by Finite Volume Methods Using Runge-Kutta Time Stepping Schemes," AIAA Paper 81-1259, June 1981.
- <sup>15</sup> Jameson, A., "Steady State Solution of the Euler Equations for Transonic Flow," Transonic, Shock and Multidimensional Flows: Advances in Scientific Computing, R. E. Meyer, ed., Academic Press, NY, 1982, pp. 37-70.
- <sup>16</sup> Jameson, A., "Solution of the Euler Equations for Two Dimensional Transonic Flow by a Multigrid Method," Applied Mathematics and Computation, vol. 13, no. 3-4, 1983, pp. 327-356.



<b>REPORT DOCUMENTATION PAGE</b>			<i>Form Approved</i> OMB No. 0704-0188	
Public reporting burden for this collection of information is estimated to average 1 hour per response, including the time for reviewing instructions, searching existing data sources, gathering and maintaining the data needed, and completing and reviewing the collection of information. Send comments regarding this burden estimate or any other aspect of this collection of information, including suggestions for reducing this burden, to Washington Headquarters Services, Directorate for Information Operations and Reports, 1215 Jefferson Davis Highway, Suite 1204, Arlington, VA 22202-4302, and to the Office of Management and Budget, Paperwork Reduction Project (0704-0188), Washington, DC 20503.				
<b>1. AGENCY USE ONLY (Leave blank)</b>	<b>2. REPORT DATE</b> April 1992	<b>3. REPORT TYPE AND DATES COVERED</b> Technical Memorandum		
<b>4. TITLE AND SUBTITLE</b> A Two-Dimensional Euler Solution for an Unbladed Jet Engine Configuration			<b>5. FUNDING NUMBERS</b>  WU-505-62-21	
<b>6. AUTHOR(S)</b> Mark E.M. Stewart				
<b>7. PERFORMING ORGANIZATION NAME(S) AND ADDRESS(ES)</b>  National Aeronautics and Space Administration Lewis Research Center Cleveland, Ohio 44135-3191			<b>8. PERFORMING ORGANIZATION REPORT NUMBER</b>  E-6691	
<b>9. SPONSORING/MONITORING AGENCY NAMES(S) AND ADDRESS(ES)</b>  National Aeronautics and Space Administration Washington, D.C. 20546-0001			<b>10. SPONSORING/MONITORING AGENCY REPORT NUMBER</b>  NASA TM-105329 ICOMP-91-22	
<b>11. SUPPLEMENTARY NOTES</b> Prepared for the Third Canadian Symposium on Aerodynamics sponsored by the Canadian Aeronautics and Space Institute, Toronto, Canada, November 20-21, 1991. Mark E.M. Stewart, Institute for Computational Mechanics in Propulsion, NASA Lewis Research Center (work funded under Space Act Agreement C99066G). Space Act Monitor: Louis A. Povinelli, (216) 433-5818.				
<b>12a. DISTRIBUTION/AVAILABILITY STATEMENT</b>  Unclassified - Unlimited Subject Category 34			<b>12b. DISTRIBUTION CODE</b>	
<b>13. ABSTRACT (Maximum 200 words)</b>  A two-dimensional, nonaxisymmetric Euler solution in a geometry representative of a jet engine configuration without blades is presented. The domain, including internal and external flow, is covered with a multiblock grid. In order to construct this grid, a domain decomposition technique is used to subdivide the domain, and smooth grids are dimensioned and placed in each block. The Euler solution is verified by examining five theoretical properties. The result demonstrates techniques for performing numerical solutions in complex geometries and provides a foundation for complete engine throughflow calculations.				
<b>14. SUBJECT TERMS</b> Computational fluid dynamics; Grid generation; Jet engines; Euler solutions			<b>15. NUMBER OF PAGES</b> 10	
			<b>16. PRICE CODE</b> A02	
<b>17. SECURITY CLASSIFICATION OF REPORT</b> Unclassified	<b>18. SECURITY CLASSIFICATION OF THIS PAGE</b> Unclassified	<b>19. SECURITY CLASSIFICATION OF ABSTRACT</b> Unclassified	<b>20. LIMITATION OF ABSTRACT</b>	